Journal of Nuclear Medicine, published on March 13, 2020 as doi:10.2967/jnumed.119.240366

OpenDose: open access resources for nuclear medicine dosimetry

Authors:

Maxime Chauvin[1], Damian Borys[2], Francesca Botta[3], Pawel Bzowski[2], Jérémie Dabin[4], Ana M. Denis-Bacelar[5], Aurélie Desbrée[6], Nadia Falzone[7,8], Boon Quan Lee[7,8], Andrea Mairani[9,10], Alessandra Malaroda[11,12], Gilles Mathieu[13], Erin McKay[14], Erick Mora-Ramirez[1,15], Andrew P. Robinson[5,16,17], David Sarrut[18], Lara Struelens[4], Alex Vergara Gil[1] and Manuel Bardiès[1,*]

and the OpenDose collaboration:

Ernesto Amato[19], Lucrezia Auditore[19], Sorina Camarasu-Pop[18], Frederic Cervenansky[18], José M. Clavijo[20], Marco A. Coca Pérez[21], Marta Cremonesi[3], José M. Fernández-Varea[22], Ludovic Ferrer[23], Telma C. F. Fonseca[24], Didier Franck[6], Silvano Gnesin[25], Antonio Italiano[26], Nico Lanconelli[27], Kamil Matusik[2], Massimiliano Pacilio[28], Isabelle Perseil[13], Daniele Pistone[29], Janick Rüegger[30], Leonel A. Torres Aroches[20] and Thiago V.M. Lima[25,30].

Affiliations:

[1] CRCT, UMR 1037, Inserm, Université Toulouse III Paul Sabatier, Toulouse, France

[2] Silesian University of Technology, Gliwice, Poland

[3] Medical Physics Unit, IEO, European Institute of Oncology IRCCS, Milan

[4] SCK•CEN, Belgian Nuclear Research Centre, Boeretang 200, 2400 Mol, Belgium

[5] National Physical Laboratory, Hampton Road, Teddington, UK

[6] Institut de Radioprotection et de Sûreté Nucléaire (IRSN), Fontenay-aux-Roses, France

[7] MRC Oxford Institute for Radiation Oncology, University of Oxford, Oxford, United Kingdom

[8] GenesisCare, Sydney, Australia

[9] Heidelberg Ion-Beam Therapy Center (HIT), Department of Radiation Oncology, Heidelberg University Hospital, Heidelberg, Germany

[10] National Centre of Oncological Hadrontherapy (CNAO), Medical Physics, Pavia, Italy

[11] School of Physics & CMRP, University of Wollongong, Wollongong, Australia

[12] Theranostic and Nuclear Medicine Department, St Vincent's Public Hospital, Sydney, Australia

[13] Inserm, Département du Système d'Information, Paris, France

[14] St George Hospital, Sydney, Australia

[15] CICANUM, Escuela de Física, Universidad de Costa Rica, San Jose, Costa Rica

[16] The University of Manchester, Manchester, UK

[17] The Christie NHS Foundation Trust, Manchester, UK

[18] Université de Lyon, CREATIS; CNRS UMR 5220; Inserm U1044; INSA-Lyon; Université Lyon 1; Centre Léon Bérard, France.

[19] Department of Biomedical and Dental Sciences and of Morphologic and Functional Imaging, University of Messina, Messina, Italy

[20] Centro de Isótopos, La Habana, Cuba

[21] MEDSCAN, Nuclear Medicine and PET/CT Centre, Concepción, Chile

[22] Facultat de Física, Universitat de Barcelona, Barcelona, Spain

[23] Institut de Cancérologie de l'Ouest, St Herblain, France

[24] Post-Graduate Program in Nuclear Sciences and Techniques of the Department of Nuclear Engineering at the UFMG in Belo Horizonte - MG Brazil

[25] Institute of Radiation Physics, Lausanne University Hospital and University of Lausanne, Lausanne, Switzerland

[26] Istituto Nazionale di Fisica Nucleare, Sezione di Catania, Italy

[27] University of Bologna, Bologna, Italy

[28] Azienda Ospedaliera Universitaria Policlinico Umberto I, Roma, Italy

[29] Department of Mathematics, Computer Science, Physics and Earth Science, University of Messina, Messina, Italy

[30] Kantonsspital Aarau, Aarau, Switzerland

First author:

Maxime Chauvin,

2 Avenue Hubert Curien, 31100 Toulouse, France

maxime.chauvin@inserm.fr

***Corresponding author:**

Manuel Bardiès,

2 Avenue Hubert Curien, 31100 Toulouse, France

manuel.bardies@inserm.fr

Short running title:

The OpenDose collaboration

Word count of the manuscript: 4855

ABSTRACT

Background: Radiopharmaceutical dosimetry depends on the localization in space and time of radioactive sources and requires the estimation of the amount of energy emitted by the sources deposited within targets. In particular, when computing resources are not accessible, this task can be carried out using precomputed tables of Specific Absorbed Fractions (SAFs) or *S values* based on dosimetric models. The OpenDose collaboration aims to generate and make freely available a range of dosimetric data and tools.

Methods: OpenDose brings together resources and expertise from 18 international teams to produce and compare traceable dosimetric data using 6 of the most popular Monte Carlo codes in radiation transport (EGSnrc/EGS++, FLUKA, GATE, Geant4, MCNP/MCNPX and PENELOPE). SAFs are uploaded, together with their associated statistical uncertainties, in a relational database. *S values* are then calculated from mono-energetic SAFs, based on the radioisotope decay data presented in the International Commission on Radiological Protection (ICRP) publication 107.

Results: The OpenDose collaboration produced SAFs for all source regions and targets combinations of the two ICRP 110 adult reference models. SAFs computed from the different Monte Carlo codes were in good agreement at all energies, with standard deviations below individual statistical uncertainties. Calculated *S values* were in good agreement with OLINDA 2 (commercial) and IDAC 2.1 (free) software. A dedicated website (www.opendose.org) has been developed to provide easy and open access to all data.

Conclusion: The OpenDose website allows the display and download of SAFs and the corresponding *S values* for 1252 radionuclides. The OpenDose collaboration, open to new research teams, will extend data production to other dosimetric models and implement new free features, such as online dosimetric tools and patient-specific absorbed dose calculation software, together with educational resources.

Keywords: nuclear medicine; dosimetry; open-access database; Monte Carlo methods.

INTRODUCTION

The necessity of dosimetry in nuclear medicine is increasingly growing with the remarkable development of targeted radionuclide therapy (*1*).

Absorbed doses in nuclear medicine are usually calculated using the Medical Internal Radiation Dose formalism (*2*), with the time-independent formulation:

$$D_{(Target,T_D)} = \sum_{Source} \tilde{A}_{(Source,T_D)} \times S_{(Target \leftarrow Source)} \quad (1)$$

where $D_{(Target,T_D)}$ is the mean absorbed dose (Gy) delivered to target tissue, $\tilde{A}_{(Source,T_D)}$ is the total number of nuclear transformations in the source (Bq·s), $S_{(Target \leftarrow Source)}$ is the mean absorbed dose to a given target per nuclear disintegration in the source (*S value*, Gy·Bq^{-1}·s^{-1}), and T_D is the dose-integration period after administration of the radioactive material. *S values* are obtained from reference human models and used for model-based dosimetry or adjusted to the geometry of a specific patient (*3*). The calculation of *S values* (Eq. 2) requires a clear definition of the geometry of the model and isotope decay characteristics:

$$S_{(Target \leftarrow Source)} = \sum_i \; E_i Y_i \Phi_{i(Target \leftarrow Source,E_i)} \quad (2)$$

where $\Phi_{i(Target \leftarrow Source,E_i)}$ is the Specific Absorbed Fraction (SAF, kg^{-1}) for radiation type i and E_i, Y_i are the energy (J) and yield (Bq^{-1}·s^{-1}) of radiation type i.

Historically, SAFs and *S values* were computed from mathematical models and were the basis for International Commission on Radiological Protection (ICRP) reports for radiopharmaceutical dosimetry (*4*). Since the publication of its report 103 (*5*), the ICRP recommends using voxel-based models, such as those presented in ICRP report 110 (*6*). This

is a logical evolution that accounts for the increasing availability of refined description of human geometry. In addition, recent developments propose polygonal mesh models (*7*), that can overcome voxel-based model limitations in the description of thin structures like organ walls.

For decades, the reference S values for mathematical models were included in MIRDOSE, then in OLINDA/EXM (http://www.doseinfo-radar.com). They were easily accessible, and most dosimetric results presented to the Food and Drug Administration or European Medicines Agency for approval of a new radiopharmaceutical were obtained using these codes. Nowadays, OLINDA/EXM 1.0 is no longer available, and OLINDA/EXM 2.0 is part of Hermes Medical Solution (http://vueinnovations.com/olinda). Moreover, SAFs and S values are no longer available on the Radiation Dose Assessment Resource website.

Recently, the ICRP Report 133 (*8*) presented SAFs for 79 sources and 43 targets of the ICRP report 110 computational models. Based on this data set, Andersson M. et al. (*9*) proposed IDAC-Dose 2.1, a desktop software to perform absorbed dose calculations.

SAFs are generated through intensive Monte Carlo simulations requiring substantial computational power. As a consequence, there is a delay between the publication of a model and its corresponding SAFs of the order of years. This delay might amplify in the coming years as the number of models and their level of complexity increases (*10*).

The OpenDose project is based on the idea that a collaborative approach enables this challenge to be addressed by offering a responsive network of shared dosimetric resources and expertise from several teams involved in radiopharmaceutical dosimetry. This allows the production and comparison of data with different codes, increasing the robustness of the

results. The OpenDose collaboration strives to produce and disseminate dosimetric data that is traceable, reproducible, and with associated uncertainties (*11*).

MATERIALS AND METHODS

The collaboration

The first meeting of the collaboration was held at the European Association of Nuclear Medicine Congress in Barcelona in 2016. This meeting defined the structure of the OpenDose collaboration and its scientific priorities, it drafted the collaboration agreement where the teams committed to generate freely accessible dosimetric data that meet the FAIR principles (*12*).

OpenDose currently includes 18 research teams over 30 institutes and has a steering committee composed of one representative per team. The collaboration organizes annual meetings to present results and discuss future actions.

The framework

A common framework (Fig. 1) has been defined to harmonize the different Monte Carlo codes and different units and formats used by the teams. Within this framework, each team is responsible for their own Monte Carlo simulations but uses the same input models and delivers the data in a common output format. Therefore, each collaboration member can independently contribute to data generation. The data produced is then collected and centralized in a database along with the models and radioisotope decay data. A dedicated

website allows access to the database, displays SAFs, calculates *S values* and allows the download of the results.

Details of the OpenDose framework are given in the sections below.

Models and radioisotope decay data

The first models considered within the collaboration are those defined in ICRP publication 110 (*6*). These voxel-based models represent the average anatomy of male and female subjects. The adult female is described by 299 x 137 x 348 voxels of size 1.775 x 1.775 x 4.84 mm^3, corresponding to a height of 1.63 m and a mass of 60 kg. The adult male is described by 254 x 127 x 222 voxels of size 2.137 x 2.137 x 8.0 mm^3, corresponding to a height of 1.76 m and a mass of 73 kg.

These models comprise 141 segmented regions (~20,000 target←source combinations) and 53 different media. As uncertainties from different regions cannot be summed post-simulation, since deposited energies in adjacent regions are likely to be correlated, 31 compound regions were added to regroup parts of an organ (e.g. kidneys are composed of regions 89 to 94). These additional 31 compound regions are the same as the target compound regions and "Total body except organ contents" defined in Table D.1 and C.1 of ICRP publication 110, respectively (*6*).

The radioisotope decay data of ICRP publication 107 (*13*) was considered for *S values* calculation. It provides electronic data for 1252 radioisotopes.

The Monte Carlo simulations and Specific Absorbed Fractions

The variety of the research teams offers a broad experience over 6 of the most widely used Monte Carlo codes in radiopharmaceutical dosimetry: EGSnrc/EGS++ (*14*), FLUKA (*15*), GATE (*16*), Geant4 (*17*), MCNP/MCNPX (*18*) and PENELOPE (*19*). These codes come from different research fields and implement different approaches to simulate radiation transport in matter, effectively offering the independent production of data. This allows verification of the production pipeline and increases data robustness.

Monte Carlo simulations estimate energy deposition in the models as a function of source location, particle type and energy. Source location can be any region of the selected model, from which particles are emitted isotropically. Monte Carlo simulations were performed for mono-energetic photons and electrons. A list of 91 energies ranging from 5 keV to 10 MeV was defined following the logarithmic energy distribution of beta emitters in ICRP 107 (*13*). Physics models, the use of variance reduction techniques and any other parameters are the choice of each team. However, to ensure data traceability and reproducibility, each team has to keep track of all simulation parameters and files. A number of 10^8 primary particles is recommended, as a trade-off between good statistics and computation time. Statistical uncertainties are estimated for all quantities (energy deposited, absorbed dose) during the runtime of the simulations using the history by history method (*20*). Each simulation provides absorbed doses and uncertainties at individual voxel-level (as binary matrices) as well as for target regions (as ASCII files).

From the simulated absorbed dose to the targets, SAFs are calculated by dividing the absorbed dose by the initial energy (J) of the particle and by the number of simulated

particles. Each team records the SAFs (and corresponding uncertainties) in a specific CSV format with a specific naming convention to ease the integration into the database.

The database

SAFs are stored in a relational SQL database as a function of parameters such as model (name, version), source / target (name, volume, mass), particle type, energy, and number of simulated particles. In addition to these parameters, data provenance (contact name, date) is also stored to ensure traceability. The radioisotope decay data is also stored in the database to enable the calculation of *S values*.

The *S value* calculation

A Python script was developed to calculate *S values* from SAFs, for any radioisotope, following equation 2. First, SAFs are extracted from the database and averaged over all Monte Carlo codes, increasing the robustness of the calculation. Then, SAFs are linearly interpolated to the energy of each radiation type of the radioisotope considered and multiplied by the corresponding yield ($Bq^{-1} \cdot s^{-1}$) and energy (J). For beta emission spectra, SAFs are integrated over energy bins. Alpha particles and alpha recoil nuclei are considered to deposit their energy locally. Finally, all emission contributions are summed to obtain the *S value* for a selected model, source, target and radioisotope. The *S value* is also calculated per particle type (photon, electron, alpha) to provide more insight on the *S value* composition.

At each step of the calculation, the uncertainty of the *S value* is computed as:

$$u(S_{(Target \leftarrow Source)})^2 = \sum_i \left(E_i Y_i u(\Phi_{i(Target \leftarrow Source, E_i)})\right)^2 \quad (3)$$

where E_i and Y_i are the energy (J) and yield ($Bq^{-1} \cdot s^{-1}$) respectively of radiation type i (for a given isotope) and $u(\Phi_{i(Target \leftarrow Source, E_i)})$ is the SAF statistical uncertainty (kg^{-1}) for radiation type i.

The computation is performed on demand to use the most up-to-date data (SAFs and nuclear data). No *S values* are stored in the database.

The website

A dedicated website was developed to provide access to all OpenDose data. A website has the advantage of being easily accessible on every device (without any installation) and easy to keep up to date.

Verification of produced data

In order to assess the variability of results amongst the different Monte Carlo codes, comparisons were carried out using one model for a restricted number of sources and energies. SAFs were computed by all teams for the ICRP 110 adult female model using Liver and Blood Vessels Trunk as sources, and monoenergetic photons and electrons of 0.05, 0.1, 0.2, 0.5, 1, 2 and 5 MeV. The liver was chosen for its relevance in radiopharmaceutical dosimetry and its compact shape, while the blood vessels of the trunk were chosen to test a more spatially complex source.

The SAFs for the source Liver were compared with the data published in ICRP 133 (*8*).

In order to calculate *S values* from the SAFs (see equation 2), the database has to contain at least one value for each model, source, target and energy combination. To ensure this, simulations were run with a reduced number of 10^7 particles with Geant4 10.5 to reach a complete data set. *S values* for a source located in the Liver of the female model, 6 targets and 3 radioisotopes commonly used in nuclear medicine (^{131}I, ^{177}Lu and ^{90}Y) were compared to IDAC-Dose 2.1 (*9*) and OLINDA/EXM 2.0 (*21*).

RESULTS

Current production status

Producing a complete data set for one model (e.g. the ICRP 110 adult female), requires ~30,000 simulations, which represents ~750,000 CPU hours of computation. By sharing the workload and the computing resources from the teams (https://www.ziemowit.hpc.polsl.pl/en, https://cc.in2p3.fr/en, https://www.calmip.univ-toulouse.fr, https://nci.org.au), the collaboration can produce data for a model in a few months. Some developments have also been made to take advantage of large grid infrastructures (*22*).

As of October 2019, the database holds 11,177,347 entries which represents data spread over 2 models, 141 sources, 172 targets, 2 particle types (photons and electrons) and 91 energies produced with 9 different Monte Carlo code versions.

Verification of produced data

For photons, SAFs from all the teams are in good agreement at all energies for both sources. For example, SAFs for Liver ← Blood Vessels Trunk present a relative standard deviation ranging from 0.67% at 5 keV to 0.23% at 5 MeV, and from 0.69% at 5 keV to 0.16% at 5 MeV for Spleen ← Liver. For electrons, SAFs have higher statistical fluctuations, especially at low energy and for targets at large distances from the source. In particular, statistical uncertainties of SAFs for Brain ← Liver are close to 100% under 200 keV. As a consequence, the SAF standard deviation between the different Monte Carlo codes can reach 65.34% for Brain ← Liver and electrons of 100 keV, and down to 1.56% at 5 MeV. It should be noted that these high relative differences correspond to negligible absolute differences. For the target Spleen that is closer to the Liver, the relative standard deviations range from 22.86% at 5 keV to 2.0% at 5 MeV.

SAFs from this preliminary assessment were also compared with data published in ICRP 133 (*8*). The agreement between OpenDose and ICRP 133 values is overall good with a mean relative difference of 1.65% for photons and 8.2% for electrons above 200 keV. However, some large differences can be noticed for low energy electrons with a maximum relative difference of +120% for Thyroid ← Liver at 100 keV. This high difference is likely due to high statistical fluctuations in the data. Unfortunately, no information on the SAF uncertainties is given in the ICRP 133. ICRP 133 values for the Brain ← Liver at energies below 200 keV are equal to 0.0, which may indicate a lower statistical power of the ICRP 133 simulations compared with the OpenDose data. These mean relative differences do not include Liver ← Liver SAF values, for which a systematic difference of 22% was found. This

is explained by the modification of some target masses in ICRP 133 (Tables A.1 and A.2 from (*8*)) to add blood content, where the original 1.400 kg Liver in the ICRP 110 adult female model has been changed to 1.810 kg.

SAF values from a selection of different Monte Carlo codes are available in Supplemental Tables 1–8, along with SAFs from ICRP 133 for comparison. The "OpenDose mean" gives the mean and standard deviation of all the available Monte Carlo codes values.

S values are available for the 2 models, 141 sources, 172 targets and 1252 radioisotopes considered so far within the collaboration OpenDose. Table 1 shows *S values* obtained for the adult female model and the comparison with IDAC-Dose 2.1 (*9*) and OLINDA/EXM 2.0 (*21*). In general, a good agreement was found. In particular, OpenDose and IDAC 2.1 values are very close which is expected since they use the same input model (ICRP 110) whereas OLINDA 2 values are calculated for a Non-Uniform Rational Basis Spline adult female model based on ICRP 89 (*23*). One can notice a systematic difference with IDAC 2.1 for Liver ← Liver, explained by the mass adjustment made in the ICRP 133 SAF calculation.

The website

The OpenDose website is online at www.opendose.org. It provides information on the project, allows to access the SAFs database and to calculate *S values* for 1252 radionuclides. Results are displayed with interactive plots and can be downloaded in CSV format. Fig. 2 shows the SAF section of the website, with results from all the Monte Carlo codes. The available data should be used for research purposes only and the website content is licensed under a Creative Commons Attribution-ShareAlike 4.0 International License.

DISCUSSION

The generation of dosimetric data represents a computing challenge, due to the resources and time required to perform simulations. The idea of a collaborative framework designed for this purpose required a preliminary verification of the precision of the dosimetric estimations of the different Monte Carlo codes used within the community.

The comparison exercise proposed to members of the collaboration, demonstrated that SAFs produced with the different Monte Carlo codes exhibit low dispersion and are in good agreement with published ICRP 133 data. The uncertainties of the SAFs and/or the *S values* estimated by OpenDose are a good indicator of the limitations of the values themselves. For example, data for electrons of low energy shows statistical limitations for targets far from the source. This information is not present in any other published SAF data. Calculated *S values* also show a good agreement with IDAC 2.1, which uses the same model and radioisotope decay scheme. OpenDose and IDAC 2.1 *S values* differ only for some sources where ICRP integrated organ mass adjustments. OpenDose decided to provide data corresponding to the models used in the Monte Carlo simulations, without any mass adjustments to avoid any calculation approximation or radiation transport simplifications and to keep a strict framework for data traceability and reproducibility.

The decay data presented in ICRP publication 107 does not include corresponding standard uncertainties, so the reported standard uncertainty of the *S value* (equation 3) is purely statistical. It should be noted that for many common radionuclides used in nuclear medicine the uncertainties on the decay data can be the dominant source of uncertainty in

the *S value* and should be included in any uncertainty estimation (*24*). In the future, OpenDose will use nuclear data with reported standard uncertainties (*25*).

During the last meeting (Oct 2019), the steering committee has decided to include, as part of the OpenDose collaboration products, two open-source software currently under development. The first implements model-based dosimetry and will be integrated in a future section of the website, while the second implements patient-specific dosimetry in a 3DSlicer (https://www.slicer.org) extension and will be available for download.

OpenDose's future vision is to make the website a *global resource* for internal dosimetry, including dosimetric data, software, and education.

CONCLUSION

The OpenDose project aims to establish a long-term international collaboration to generate an open access database for nuclear medicine dosimetry. The collaboration includes 18 teams with expertise in radiopharmaceutical dosimetry, Monte Carlo methods and high-performance computing. The initial task set for all partners to produce a set of simulations for a specific model allowed the definition of a common computational framework and to establish a unified results format. OpenDose has now produced SAFs and uncertainties for the two ICRP 110 adult models, covering all source-target combinations, 2 particle types (photon and electron) and 91 energies. Data production will continue and extend to other computational models.

The dedicated website is online at www.opendose.org. It allows easy access to the SAF database and the calculation of *S values* for 1252 radionuclides. *S values* generated for

the models considered so far are close to those already available in the literature. A new website section is under-development to perform model-based dosimetry calculations.

The collaboration is open to new research teams willing to participate in any OpenDose related activity, from the production of dosimetric data to the development of the website and dosimetry tools.

DISCLOSURE

No potential conflicts of interest relevant to this article exist.

ACKNOWLEDGEMENTS

This work was supported by the National Measurement System of the UK's Department for Business, Energy and Industrial Strategy.

This work was performed within the framework of the SIRIC LYriCAN Grant INCa-INSERM-DGOS-12563, and the LABEX PRIMES (ANR-11-LABX-0063) of Université de Lyon, within the program Investissements d'Avenir (ANR- 11-IDEX-0007) operated by the ANR.

The authors acknowledge the support of France Grilles, the EGI infrastructure, the biomed virtual organization and the Virtual Imaging Platform for providing computing resources and services.

Part of this work was supported by the Euratom research and training program, 2014–2018, under grant agreement No 755523 (MEDIRAD).

Calculations were partially performed on the Ziemowit computer cluster in the Laboratory of Bioinformatics and Computational Biology (Silesian University of Technology), created in the EU Innovative Economy Program POIG.02.01.00-00-166/08 and expanded in the POIG.02.03.01-00-040/13 project.

This project was undertaken with the assistance of resources and services from the National Computational Infrastructure (NCI), which is supported by the Australian Government.

The authors acknowledge Yves-Marie Gouesnard for his contribution to the website.

KEY POINTS

QUESTION:

Can we facilitate the practice of dosimetry in Nuclear Medicine?

PERTINENT FINDINGS:

The OpenDose collaboration brings together the resources and expertise of many research teams involved in radiopharmaceutical dosimetry. The www.opendose.org website provides a *global repository* for internal dosimetry, including data, software, and education material.

IMPLICATIONS FOR PATIENT CARE:

The OpenDose project will help the practice of internal dosimetry by providing open-access resources.

REFERENCES

1. Stokke C, Gabiña PM, Solný P, et al. Dosimetry-based treatment planning for molecular radiotherapy: a summary of the 2017 report from the Internal Dosimetry Task Force. *EJNMMI Phys*. 2017;4:27.

2. Bolch WE, Eckerman KF, Sgouros G, et al. MIRD pamphlet No. 21: A generalized schema for radiopharmaceutical dosimetry-standardization of nomenclature. *J Nucl Med*. 2009;50:477-484.

3. Divoli A, Chiavassa S, Ferrer L, Barbet J, Flux GD, Bardiès M. Effect of patient morphology on dosimetric calculations for internal irradiation as assessed by comparisons of Monte Carlo versus conventional methodologies. *J Nucl Med*. 2009;50:316-323.

4. ICRP. Radiation dose to patients from radiopharmaceuticals: a compendium of current information related to frequently used substances. ICRP publication 128. *Ann ICRP*. 2015;44:7-321.

5. ICRP. The 2007 recommendations of the International Commission on Radiological Protection. ICRP publication 103. *Ann ICRP*. 2007;37:1-332.

6. ICRP. Adult reference computational phantoms. ICRP publication 110. *Ann ICRP*. 2009;39:1-164.

7. Kim CH, Yeom YS, Nguyen TT, et al. New mesh-type phantoms and their dosimetric applications, including emergencies. *Ann ICRP*. 2018;47:45-62.

8. ICRP. The ICRP computational framework for internal dose assessment for reference adults: specific absorbed fractions. ICRP publication 133. *Ann ICRP*. 2016;45:5-73.

9. Andersson M, Johansson L, Eckerman K, Mattsson S. IDAC-Dose 2.1, an internal dosimetry program for diagnostic nuclear medicine based on the ICRP adult reference voxel phantoms. *EJNMMI Res*. 2017;7:88.

10. Xu XG. An exponential growth of computational phantom research in radiation protection, imaging, and radiotherapy: a review of the fifty-year history. *Phys Med Biol*. 2014;59:R233-R302.

11. Gear JI, Cox MG, Gustafsson J, et al. EANM practical guidance on uncertainty analysis for molecular radiotherapy absorbed dose calculations. *Eur J Nucl Med Mol Imaging*. 2018;45:2456-2474.

12. Wilkinson MD, Dumontier M, Aalbersberg IjJ, et al. The FAIR Guiding Principles for scientific data management and stewardship. *Sci Data*. 2016;3:160018.

13. ICRP. Nuclear decay data for dosimetric calculations. ICRP publication 107. *Ann ICRP*. 2008;38:7-96.

14. Kawrakow I, Mainegra-Hing E, Rogers DWO, Tessier F, Walters BRB. The EGSnrc code system: Monte Carlo simulation of electron and photon transport. *Tech Rep PIRS-701, Natl Res Counc Canada*. 2017.

15. Böhlen TT, Cerutti F, Chin MPW, et al. The FLUKA code: developments and challenges for high energy and medical applications. *Nucl Data Sheets*. 2014;120:211-214.

16. Sarrut D, Bardiès M, Boussion N, et al. A review of the use and potential of the GATE Monte Carlo simulation code for radiation therapy and dosimetry applications. *Med Phys*. 2014;41:64301.

17. Agostinelli S, Allison J, Amako K, et al. Geant4—a simulation toolkit. *Nucl Instruments Methods Phys Res Sect A Accel Spectrometers, Detect Assoc Equip*. 2003;506:250-303.

18. Waters LS, McKinney GW, Durkee JW, et al. The MCNPX Monte Carlo radiation transport code. In: AIP Conference Proceedings. Vol 896. ; 2007:81-90.

19. Salvat F, Fernandez-Varea JM, Sempau J. PENELOPE-2011: a code system for Monte Carlo simulation of electron and photon transport. OECD Nuclear Energy Agency; 2014.

20. Walters BRB, Kawrakow I, Rogers DWO. History by history statistical estimators in the BEAM code system. *Med Phys*. 2002;29:2745-2752.

21. Stabin MG, Siegel JA. RADAR dose estimate report: a compendium of radiopharmaceutical dose estimates based on OLINDA/EXM Version 2.0. *J Nucl Med*. 2018;59:154-160.

22. Chauvin M, Mathieu G, Camarasu-Pop S, Bonnet A, Bardies M, Perseil I. Enabling large scale data production for OpenDose with GATE on the EGI infrastructure. In: 2019 19th IEEE/ACM International Symposium on Cluster, Cloud and Grid Computing (CCGRID). IEEE; 2019:658-665.

23. ICRP. Basic anatomical and physiological data for use in radiological protection reference values. ICRP publication 89. *Ann ICRP*. 2002;32:1-277.

24. JCGM. JCGM 100: evaluation of measurement data - guide to the expression of uncertainty in measurement.; 2008.

25. Tuli JK. Evaluated Nuclear Structure Data File -- a manual for the preparation of data sets. Upton, NY; 2001.

Figures

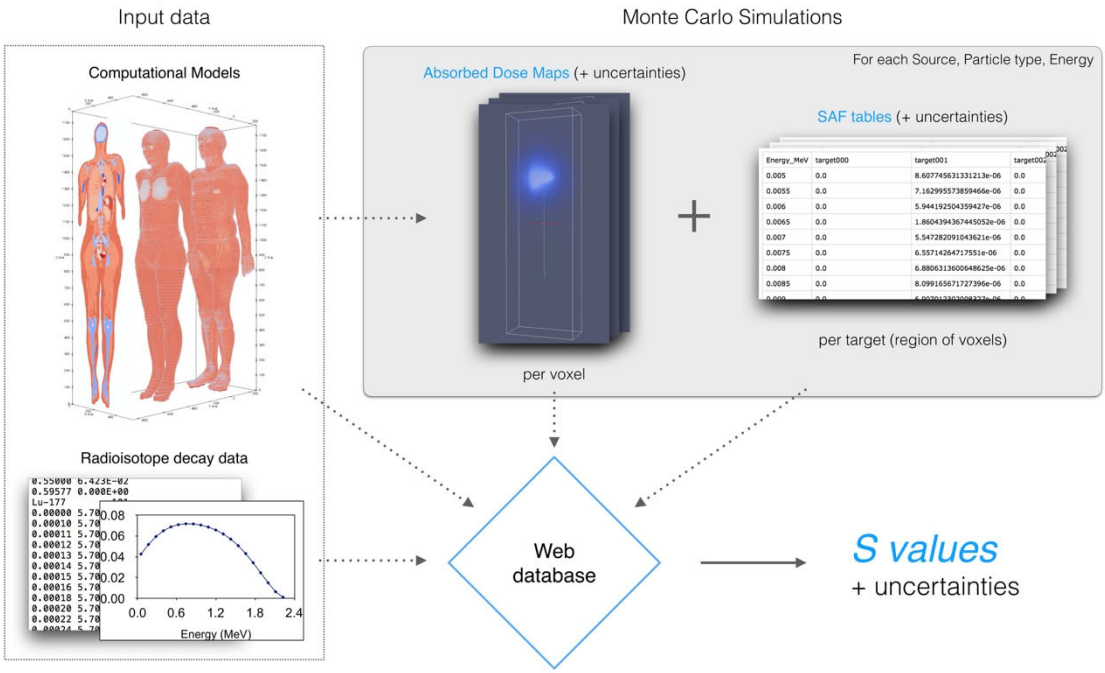

FIGURE 1. The OpenDose framework. The SAFs produced by Monte Carlo simulations are stored in a database along with the input data. A web application allows to calculate, display and download SAFs and *S values*.

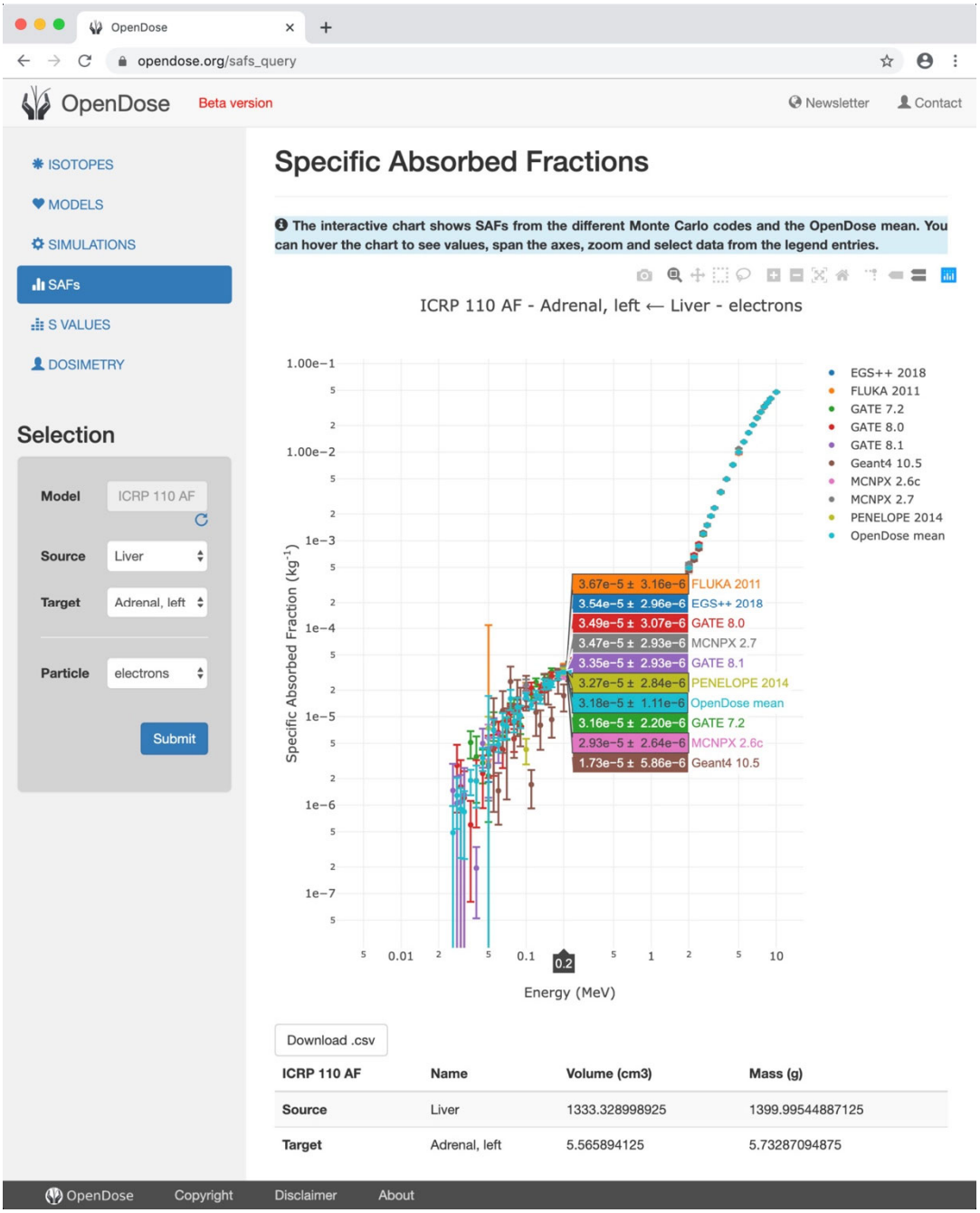

FIGURE 2. The SAFs section of the OpenDose website allows the display and download of data from all the Monte Carlo codes.

Tables

Target	^{131}I			^{177}Lu			^{90}Y		
	OpenDose	IDAC 2.1	OLINDA 2	OpenDose	IDAC 2.1	OLINDA 2	OpenDose	IDAC 2.1	OLINDA 2
Brain	1.492e-8 ± 9.5e-11	1.46e-8 -	1.47e-8 -	8.423e-10 ± 4.6e-12	8.44e-10 -	8.10e-10 -	1.084e-10 ± 2.6e-12	1.08e-10 -	4.27e-11 -
Gallbladder wall	6.355e-6 ± 1.2e-8	6.33e-6 -	2.43e-6 -	1.100e-6 ± 2.8e-9	1.09e-6 -	2.52e-7 -	2.228e-5 ± 2.5e-8	2.20e-5 -	5.16e-8 -
Liver	2.842e-5 ± 4.7e-9	2.20e-5 -	2.89e-5 -	1.753e-5 ± 1.3e-9	1.36e-5 -	1.76e-5 -	1.015e-4 ± 7.7e-9	7.83e-5 -	1.03e-4 -
Pancreas	2.165e-6 ± 2.9e-9	2.18e-6 -	2.15e-6 -	2.255e-7 ± 5.0e-10	2.27e-7 -	2.34e-7 -	4.518e-7 ± 1.3e-9	4.61e-7 -	1.54e-6 -
Spleen	7.654e-7 ± 1.7e-9	7.69e-7 -	4.12e-7 -	7.655e-8 ± 2.3e-10	7.69e-8 -	3.81e-8 -	7.824e-9 ± 5.3e-11	7.94e-9 -	2.35e-9 -
Thyroid	1.443e-7 ± 4.5e-10	1.44e-7 -	1.74e-7 -	1.282e-8 ± 9.9e-11	1.29e-8 -	1.61e-8 -	1.287e-9 ± 2.8e-11	1.43e-9 -	4.86e-10 -

TABLE 1. OpenDose *S values* compared to IDAC-Dose 2.1 and OLINDA/EXM 2.0 for ^{131}I, ^{177}Lu and ^{90}Y in the Liver of the ICRP 110 female model.

Supplemental data

Target	Energy (MeV)	EGS++ 2018	FLUKA 2011	GATE 8.1	Geant4 10.5	MCNPX 2.7	PENELOPE 2014	OpenDose mean
Blood Vessels, Trunk	0.05	2.022e-01 ± 7.6e-05	2.054e-01 ± 3.7e-05	2.032e-01 ± 7.6e-05	2.038e-01 ± 2.2e-04	2.052e-01 ± 8.2e-05	2.028e-01 ± 7.6e-05	2.042e-01 ± 1.2e-03
	0.1	1.108e-01 ± 3.8e-05	1.125e-01 ± 1.9e-05	1.120e-01 ± 3.8e-05	1.122e-01 ± 1.0e-04	1.127e-01 ± 3.4e-05	1.122e-01 ± 3.7e-05	1.122e-01 ± 5.8e-04
	0.2	1.160e-01 ± 3.8e-05	1.169e-01 ± 5.7e-05	1.171e-01 ± 3.8e-05	1.162e-01 ± 1.0e-04	1.171e-01 ± 3.5e-05	1.170e-01 ± 3.7e-05	1.169e-01 ± 4.3e-04
	0.5	1.205e-01 ± 4.7e-05	1.207e-01 ± 7.4e-06	1.206e-01 ± 4.7e-05	1.211e-01 ± 5.5e-05	1.206e-01 ± 4.8e-05	1.208e-01 ± 4.4e-05	1.207e-01 ± 1.9e-04
	1	1.052e-01 ± 4.7e-05	1.051e-01 ± 7.5e-06	1.049e-01 ± 4.7e-05	1.058e-01 ± 2.4e-05	1.047e-01 ± 4.2e-05	1.053e-01 ± 3.9e-05	1.051e-01 ± 3.2e-04
	2	7.574e-02 ± 4.1e-05	7.561e-02 ± 2.2e-05	7.540e-02 ± 4.1e-05	7.567e-02 ± 1.4e-05	7.490e-02 ± 3.7e-05	7.575e-02 ± 2.6e-05	7.551e-02 ± 2.7e-04
	5	3.808e-02 ± 2.7e-05	3.817e-02 ± 6.1e-05	3.809e-02 ± 2.7e-05	3.804e-02 ± 1.1e-05	3.726e-02 ± 2.6e-05	3.809e-02 ± 1.2e-05	3.800e-02 ± 2.8e-04
Brain	0.05	2.840e-04 ± 1.3e-06	2.714e-04 ± 4.3e-07	2.766e-04 ± 1.3e-06	2.824e-04 ± 3.6e-06	2.688e-04 ± 1.3e-06	2.694e-04 ± 1.2e-06	2.743e-04 ± 5.7e-06
	0.1	5.426e-04 ± 1.4e-06	5.385e-04 ± 1.1e-06	5.392e-04 ± 1.4e-06	5.525e-04 ± 3.4e-06	5.382e-04 ± 1.4e-06	5.359e-04 ± 1.1e-06	5.409e-04 ± 4.8e-06
	0.2	6.458e-04 ± 1.3e-06	6.484e-04 ± 2.6e-06	6.499e-04 ± 1.3e-06	6.549e-04 ± 3.0e-06	6.488e-04 ± 1.4e-06	6.477e-04 ± 1.0e-06	6.497e-04 ± 2.6e-06
	0.5	8.121e-04 ± 1.6e-06	8.172e-04 ± 5.6e-07	8.171e-04 ± 1.7e-06	8.124e-04 ± 2.4e-06	8.126e-04 ± 1.6e-06	8.133e-04 ± 1.3e-06	8.144e-04 ± 2.4e-06
	1	9.206e-04 ± 1.9e-06	9.238e-04 ± 8.1e-07	9.222e-04 ± 1.9e-06	9.242e-04 ± 1.7e-06	9.226e-04 ± 1.9e-06	9.227e-04 ± 1.5e-06	9.221e-04 ± 1.6e-06
	2	9.645e-04 ± 2.1e-06	9.660e-04 ± 2.0e-05	9.618e-04 ± 2.1e-06	9.623e-04 ± 1.3e-06	9.674e-04 ± 2.1e-06	9.642e-04 ± 1.2e-06	9.645e-04 ± 2.0e-06
	5	8.956e-04 ± 2.1e-06	8.973e-04 ± 2.3e-06	8.933e-04 ± 2.1e-06	8.920e-04 ± 1.0e-06	8.971e-04 ± 2.2e-06	8.962e-04 ± 8.2e-07	8.951e-04 ± 1.9e-06
Liver	0.05	1.979e-02 ± 1.0e-05	2.011e-02 ± 3.6e-06	2.005e-02 ± 1.0e-05	2.031e-02 ± 2.9e-05	2.010e-02 ± 1.0e-05	2.004e-02 ± 9.7e-06	2.007e-02 ± 1.3e-04
	0.1	1.459e-02 ± 7.0e-06	1.487e-02 ± 1.0e-05	1.479e-02 ± 7.0e-06	1.493e-02 ± 1.6e-05	1.487e-02 ± 7.4e-06	1.483e-02 ± 5.7e-06	1.482e-02 ± 9.8e-05
	0.2	1.314e-02 ± 5.9e-06	1.325e-02 ± 9.3e-07	1.323e-02 ± 6.0e-06	1.330e-02 ± 1.3e-05	1.328e-02 ± 6.6e-06	1.325e-02 ± 4.7e-06	1.325e-02 ± 4.7e-05
	0.5	1.254e-02 ± 6.5e-06	1.258e-02 ± 3.3e-07	1.256e-02 ± 6.5e-06	1.259e-02 ± 8.0e-06	1.260e-02 ± 6.3e-06	1.258e-02 ± 5.4e-06	1.257e-02 ± 2.0e-05
	1	1.161e-02 ± 6.8e-06	1.163e-02 ± 3.5e-06	1.162e-02 ± 6.8e-06	1.169e-02 ± 4.4e-06	1.165e-02 ± 7.0e-06	1.163e-02 ± 5.1e-06	1.163e-02 ± 2.3e-05
	2	1.008e-02 ± 6.7e-06	1.009e-02 ± 2.9e-04	1.009e-02 ± 6.7e-06	1.012e-02 ± 2.6e-06	1.012e-02 ± 7.1e-06	1.011e-02 ± 3.8e-06	1.010e-02 ± 1.5e-05
	5	7.826e-03 ± 6.1e-06	7.829e-03 ± 5.6e-06	7.825e-03 ± 6.1e-06	7.793e-03 ± 1.6e-06	7.851e-03 ± 6.3e-06	7.832e-03 ± 2.2e-06	7.828e-03 ± 1.8e-05

Table 1. *OpenDose photon SAFs (kg^{-1}) for the model ICRP 110 adult female, the source Blood Vessels Trunk and target Blood Vessels Trunk, Brain and Liver. SAFs are given for a selection of different Monte Carlo codes and the mean over all available OpenDose data is also shown.*

Target	Energy (MeV)	EGS++ 2018	FLUKA 2011	GATE 8.1	Geant4 10.5	MCNPX 2.7	PENELOPE 2014	OpenDose mean
Spleen	0.05	1.776e-02 ± 3.1e-05	1.813e-02 ± 5.0e-05	1.808e-02 ± 3.2e-05	1.844e-02 ± 9.3e-05	1.810e-02 ± 3.1e-05	1.810e-02 ± 3.0e-05	1.810e-02 ± 1.7e-04
	0.1	1.309e-02 ± 1.9e-05	1.337e-02 ± 1.4e-05	1.327e-02 ± 2.0e-05	1.353e-02 ± 5.3e-05	1.333e-02 ± 2.0e-05	1.329e-02 ± 1.8e-05	1.331e-02 ± 1.1e-04
	0.2	1.156e-02 ± 1.6e-05	1.169e-02 ± 1.6e-05	1.166e-02 ± 1.6e-05	1.169e-02 ± 4.2e-05	1.168e-02 ± 1.6e-05	1.169e-02 ± 1.4e-05	1.167e-02 ± 4.0e-05
	0.5	1.087e-02 ± 1.8e-05	1.090e-02 ± 1.1e-05	1.092e-02 ± 1.8e-05	1.094e-02 ± 2.7e-05	1.092e-02 ± 1.9e-05	1.090e-02 ± 1.6e-05	1.090e-02 ± 2.6e-05
	1	1.000e-02 ± 2.0e-05	1.005e-02 ± 3.8e-05	9.985e-03 ± 1.9e-05	1.006e-02 ± 1.7e-05	1.005e-02 ± 1.9e-05	1.005e-02 ± 1.6e-05	1.003e-02 ± 2.6e-05
	2	8.697e-03 ± 1.9e-05	8.736e-03 ± 1.8e-05	8.695e-03 ± 1.9e-05	8.744e-03 ± 1.2e-05	8.705e-03 ± 1.9e-05	8.726e-03 ± 1.2e-05	8.710e-03 ± 2.4e-05
	5	6.815e-03 ± 1.7e-05	6.797e-03 ± 2.1e-05	6.803e-03 ± 1.7e-05	6.803e-03 ± 8.7e-06	6.805e-03 ± 1.7e-05	6.795e-03 ± 6.7e-06	6.798e-03 ± 1.1e-05
Thyroid	0.05	6.722e-02 ± 1.7e-04	6.869e-02 ± 3.2e-04	6.796e-02 ± 1.7e-04	7.334e-02 ± 5.1e-04	6.938e-02 ± 1.7e-04	6.765e-02 ± 1.6e-04	6.885e-02 ± 1.8e-03
	0.1	3.754e-02 ± 8.8e-05	3.778e-02 ± 1.3e-04	3.751e-02 ± 8.8e-05	3.850e-02 ± 2.5e-04	3.801e-02 ± 8.7e-05	3.765e-02 ± 8.3e-05	3.783e-02 ± 3.1e-04
	0.2	3.461e-02 ± 7.8e-05	3.460e-02 ± 8.7e-05	3.457e-02 ± 7.8e-05	3.442e-02 ± 2.1e-04	3.464e-02 ± 8.0e-05	3.454e-02 ± 7.4e-05	3.457e-02 ± 7.1e-05
	0.5	3.442e-02 ± 9.3e-05	3.428e-02 ± 1.7e-04	3.435e-02 ± 9.3e-05	3.429e-02 ± 1.3e-04	3.430e-02 ± 9.3e-05	3.432e-02 ± 8.6e-05	3.430e-02 ± 6.5e-05
	1	3.172e-02 ± 9.8e-05	3.160e-02 ± 1.4e-04	3.182e-02 ± 9.8e-05	3.238e-02 ± 8.5e-05	3.180e-02 ± 9.9e-05	3.151e-02 ± 8.0e-05	3.177e-02 ± 2.5e-04
	2	2.689e-02 ± 9.2e-05	2.715e-02 ± 4.1e-05	2.712e-02 ± 9.2e-05	2.804e-02 ± 6.2e-05	2.708e-02 ± 9.2e-05	2.698e-02 ± 5.8e-05	2.714e-02 ± 3.5e-04
	5	1.958e-02 ± 7.2e-05	1.964e-02 ± 1.2e-04	1.964e-02 ± 7.2e-05	1.939e-02 ± 4.2e-05	1.947e-02 ± 7.0e-05	1.960e-02 ± 3.2e-05	1.956e-02 ± 8.2e-05
Urinary Bladder Wall	0.05	2.722e-02 ± 6.9e-05	2.772e-02 ± 6.4e-05	2.764e-02 ± 6.9e-05	2.759e-02 ± 2.1e-04	2.773e-02 ± 6.9e-05	2.752e-02 ± 6.8e-05	2.760e-02 ± 1.6e-04
	0.1	1.699e-02 ± 3.7e-05	1.734e-02 ± 1.6e-05	1.730e-02 ± 3.8e-05	1.738e-02 ± 1.1e-04	1.740e-02 ± 3.8e-05	1.728e-02 ± 3.6e-05	1.729e-02 ± 1.2e-04
	0.2	1.585e-02 ± 3.3e-05	1.602e-02 ± 2.1e-05	1.595e-02 ± 3.3e-05	1.598e-02 ± 9.2e-05	1.611e-02 ± 3.2e-05	1.598e-02 ± 3.2e-05	1.600e-02 ± 8.2e-05
	0.5	1.569e-02 ± 3.9e-05	1.568e-02 ± 7.2e-05	1.572e-02 ± 3.9e-05	1.566e-02 ± 5.9e-05	1.569e-02 ± 3.9e-05	1.576e-02 ± 3.7e-05	1.569e-02 ± 2.9e-05
	1	1.448e-02 ± 4.0e-05	1.453e-02 ± 1.0e-04	1.447e-02 ± 4.0e-05	1.459e-02 ± 3.8e-05	1.452e-02 ± 3.9e-05	1.446e-02 ± 3.5e-05	1.450e-02 ± 4.0e-05
	2	1.229e-02 ± 3.4e-05	1.233e-02 ± 6.5e-05	1.229e-02 ± 3.4e-05	1.231e-02 ± 2.7e-05	1.235e-02 ± 3.3e-05	1.240e-02 ± 2.5e-05	1.234e-02 ± 3.8e-05
	5	8.891e-03 ± 2.4e-05	8.833e-03 ± 3.5e-07	8.858e-03 ± 2.4e-05	8.963e-03 ± 1.9e-05	8.878e-03 ± 2.3e-05	8.931e-03 ± 1.4e-05	8.897e-03 ± 3.9e-05

Table 2. *OpenDose photon SAFs (kg^{-1}) for the model ICRP 110 adult female, the source Blood Vessels Trunk and target Spleen, Thyroid and Urinary Bladder Wall. SAFs are given for a selection of different Monte Carlo codes and the mean over all available OpenDose data is also shown.*

Target	Energy (MeV)	EGS++ 2018	FLUKA 2011	GATE 8.1	Geant4 10.5	MCNPX 2.7	PENELOPE 2014	OpenDose mean
Blood Vessels, Trunk	0.05	4.111e+00 ± 2.1e-05	4.086e+00 ± 3.2e-05	4.111e+00 ± 2.2e-05	4.111e+00 ± 3.2e-04	4.110e+00 ± 0.0e+00	4.111e+00 ± 4.1e-04	4.108e+00 ± 8.2e-03
	0.1	4.078e+00 ± 3.8e-05	4.065e+00 ± 2.7e-05	4.076e+00 ± 3.9e-05	4.077e+00 ± 8.1e-04	4.074e+00 ± 0.0e+00	4.078e+00 ± 4.1e-04	4.075e+00 ± 4.0e-03
	0.2	3.980e+00 ± 6.4e-05	3.974e+00 ± 8.3e-05	3.978e+00 ± 6.5e-05	3.979e+00 ± 1.1e-03	3.972e+00 ± 0.0e+00	3.982e+00 ± 3.9e-04	3.978e+00 ± 3.3e-03
	0.5	3.614e+00 ± 1.1e-04	3.608e+00 ± 2.0e-04	3.609e+00 ± 1.1e-04	3.612e+00 ± 1.1e-03	3.591e+00 ± 0.0e+00	3.617e+00 ± 3.3e-04	3.609e+00 ± 7.6e-03
	1	3.052e+00 ± 1.4e-04	3.046e+00 ± 3.7e-04	3.044e+00 ± 1.4e-04	3.051e+00 ± 9.4e-04	3.010e+00 ± 0.0e+00	3.054e+00 ± 2.4e-04	3.044e+00 ± 1.3e-02
	2	2.262e+00 ± 1.5e-04	2.264e+00 ± 8.9e-05	2.259e+00 ± 1.5e-04	2.265e+00 ± 7.0e-04	2.210e+00 ± 2.2e-04	2.264e+00 ± 1.4e-04	2.256e+00 ± 1.8e-02
	5	1.224e+00 ± 1.1e-04	1.234e+00 ± 5.3e-05	1.231e+00 ± 1.1e-04	1.233e+00 ± 3.7e-04	1.182e+00 ± 1.2e-04	1.224e+00 ± 6.5e-05	1.224e+00 ± 1.6e-02
Brain	0.05	1.232e-09 ± 1.0e-09	6.428e-09 ± 6.4e-09	1.252e-09 ± 1.3e-09	4.599e-08 ± 4.2e-08	0.000e+00 ± 0.0e+00	4.021e-09 ± 4.1e-09	7.550e-09 ± 1.5e-08
	0.1	6.045e-08 ± 1.4e-08	5.600e-08 ± 5.3e-09	2.969e-08 ± 7.8e-09	1.765e-09 ± 1.8e-09	5.276e-08 ± 1.2e-08	5.978e-08 ± 1.1e-08	4.098e-08 ± 1.9e-08
	0.2	1.966e-07 ± 1.8e-08	2.161e-07 ± 2.4e-08	1.923e-07 ± 2.0e-08	2.775e-07 ± 6.0e-08	2.331e-07 ± 2.1e-08	1.983e-07 ± 1.7e-08	2.099e-07 ± 3.1e-08
	0.5	7.215e-07 ± 2.7e-08	7.580e-07 ± 2.8e-08	7.207e-07 ± 2.9e-08	6.542e-07 ± 5.7e-08	7.687e-07 ± 2.8e-08	6.985e-07 ± 2.2e-08	7.191e-07 ± 3.5e-08
	1	1.840e-06 ± 4.2e-08	1.888e-06 ± 3.5e-08	1.757e-06 ± 4.0e-08	1.805e-06 ± 7.2e-08	1.857e-06 ± 4.1e-08	1.861e-06 ± 3.4e-08	1.838e-06 ± 3.8e-08
	2	4.666e-06 ± 6.7e-08	4.645e-06 ± 8.4e-08	4.610e-06 ± 6.8e-08	4.325e-06 ± 8.1e-08	4.891e-06 ± 7.0e-08	4.627e-06 ± 5.2e-08	4.629e-06 ± 1.5e-07
	5	1.567e-05 ± 1.3e-07	1.611e-05 ± 8.8e-08	1.558e-05 ± 1.3e-07	1.550e-05 ± 1.0e-07	1.624e-05 ± 1.4e-07	1.555e-05 ± 8.1e-08	1.568e-05 ± 2.9e-07
Liver	0.05	1.697e-05 ± 2.9e-07	3.599e-05 ± 9.3e-08	1.740e-05 ± 3.0e-07	1.791e-05 ± 5.3e-07	1.853e-05 ± 3.1e-07	1.673e-05 ± 2.9e-07	1.938e-05 ± 6.3e-06
	0.1	5.388e-05 ± 5.2e-07	6.324e-05 ± 5.0e-07	5.620e-05 ± 5.3e-07	5.508e-05 ± 8.9e-07	5.882e-05 ± 5.4e-07	5.413e-05 ± 5.1e-07	5.636e-05 ± 3.0e-06
	0.2	1.605e-04 ± 8.9e-07	1.658e-04 ± 1.1e-06	1.621e-04 ± 8.9e-07	1.623e-04 ± 1.3e-06	1.708e-04 ± 9.1e-07	1.597e-04 ± 8.8e-07	1.630e-04 ± 3.4e-06
	0.5	5.634e-04 ± 1.6e-06	5.679e-04 ± 3.1e-07	5.739e-04 ± 1.7e-06	5.619e-04 ± 1.7e-06	5.956e-04 ± 1.7e-06	5.625e-04 ± 1.6e-06	5.715e-04 ± 1.0e-05
	1	1.290e-03 ± 2.4e-06	1.300e-03 ± 2.3e-06	1.303e-03 ± 2.4e-06	1.284e-03 ± 1.9e-06	1.351e-03 ± 2.4e-06	1.290e-03 ± 2.0e-06	1.302e-03 ± 2.0e-05
	2	3.080e-03 ± 3.7e-06	3.082e-03 ± 2.9e-06	3.111e-03 ± 3.7e-06	3.089e-03 ± 2.1e-06	3.250e-03 ± 3.9e-06	3.084e-03 ± 2.2e-06	3.111e-03 ± 5.4e-05
	5	1.007e-02 ± 6.5e-06	1.001e-02 ± 4.4e-06	1.006e-02 ± 6.5e-06	1.009e-02 ± 8.1e-07	1.051e-02 ± 6.3e-06	1.009e-02 ± 2.5e-06	1.011e-02 ± 1.5e-04

Table 3. *OpenDose electron SAFs (kg^{-1}) for the model ICRP 110 adult female, the source Blood Vessels Trunk and target Blood Vessels Trunk, Brain and Liver. SAFs are given for a selection of different Monte Carlo codes and the mean over all available OpenDose data is also shown.*

Target	Energy (MeV)	EGS++ 2018	FLUKA 2011	GATE 8.1	Geant4 10.5	MCNPX 2.7	PENELOPE 2014	OpenDose mean
Spleen	0.05	1.575e-06 ± 2.5e-07	1.241e-06 ± 6.7e-08	1.642e-06 ± 2.6e-07	1.091e-06 ± 7.3e-07	1.185e-06 ± 2.2e-07	1.524e-06 ± 2.5e-07	1.351e-06 ± 2.4e-07
	0.1	3.999e-06 ± 3.1e-07	4.454e-06 ± 5.2e-09	4.431e-06 ± 3.2e-07	3.263e-06 ± 7.9e-07	4.842e-06 ± 3.4e-07	3.925e-06 ± 3.0e-07	4.216e-06 ± 4.7e-07
	0.2	1.051e-05 ± 3.8e-07	1.101e-05 ± 1.4e-08	1.047e-05 ± 3.7e-07	1.001e-05 ± 1.1e-06	1.053e-05 ± 3.8e-07	9.672e-06 ± 3.4e-07	1.025e-05 ± 4.1e-07
	0.5	2.230e-05 ± 4.0e-07	2.418e-05 ± 5.1e-07	2.242e-05 ± 3.9e-07	2.396e-05 ± 1.1e-06	2.437e-05 ± 4.2e-07	2.232e-05 ± 3.7e-07	2.316e-05 ± 8.2e-07
	1	4.044e-05 ± 4.8e-07	4.329e-05 ± 3.8e-07	4.132e-05 ± 4.8e-07	4.120e-05 ± 1.0e-06	4.426e-05 ± 5.0e-07	4.094e-05 ± 4.5e-07	4.194e-05 ± 1.2e-06
	2	8.394e-05 ± 7.8e-07	8.988e-05 ± 5.0e-07	8.826e-05 ± 8.2e-07	8.373e-05 ± 1.1e-06	9.213e-05 ± 8.5e-07	8.634e-05 ± 6.7e-07	8.713e-05 ± 2.7e-06
	5	1.588e-03 ± 5.9e-06	1.582e-03 ± 6.2e-06	1.600e-03 ± 5.9e-06	1.606e-03 ± 3.7e-06	1.765e-03 ± 6.2e-06	1.622e-03 ± 3.3e-06	1.614e-03 ± 5.8e-05
Thyroid	0.05	3.158e-05 ± 3.3e-06	1.231e-04 ± 8.7e-06	3.320e-05 ± 3.5e-06	2.031e-05 ± 6.2e-06	3.344e-05 ± 3.5e-06	4.121e-05 ± 3.8e-06	4.273e-05 ± 3.1e-05
	0.1	9.938e-05 ± 5.8e-06	1.666e-04 ± 2.4e-06	9.510e-05 ± 5.7e-06	1.106e-04 ± 1.1e-05	1.054e-04 ± 5.9e-06	9.314e-05 ± 5.5e-06	1.067e-04 ± 2.4e-05
	0.2	2.729e-04 ± 9.7e-06	3.263e-04 ± 4.9e-06	2.637e-04 ± 9.5e-06	2.587e-04 ± 1.5e-05	2.813e-04 ± 9.7e-06	2.707e-04 ± 9.5e-06	2.738e-04 ± 2.1e-05
	0.5	1.238e-03 ± 2.1e-05	1.280e-03 ± 9.1e-06	1.241e-03 ± 2.1e-05	1.251e-03 ± 2.2e-05	1.330e-03 ± 2.1e-05	1.201e-03 ± 1.9e-05	1.253e-03 ± 3.7e-05
	1	6.444e-03 ± 4.4e-05	6.612e-03 ± 3.0e-05	6.586e-03 ± 4.4e-05	6.574e-03 ± 3.8e-05	6.997e-03 ± 4.5e-05	6.368e-03 ± 3.8e-05	6.568e-03 ± 1.9e-04
	2	3.960e-02 ± 1.1e-04	3.961e-02 ± 1.4e-05	4.028e-02 ± 1.1e-04	3.966e-02 ± 7.2e-05	4.308e-02 ± 1.1e-04	3.970e-02 ± 7.2e-05	4.021e-02 ± 1.1e-03
	5	1.411e-01 ± 2.0e-04	1.409e-01 ± 2.9e-04	1.409e-01 ± 2.0e-04	1.405e-01 ± 1.0e-04	1.454e-01 ± 2.0e-04	1.412e-01 ± 8.4e-05	1.414e-01 ± 1.6e-03
Urinary Bladder Wall	0.05	3.482e-04 ± 8.0e-06	8.495e-04 ± 2.2e-05	3.639e-04 ± 8.2e-06	3.898e-04 ± 1.4e-05	3.752e-04 ± 8.3e-06	3.551e-04 ± 8.1e-06	4.161e-04 ± 1.6e-04
	0.1	1.140e-03 ± 1.4e-05	1.254e-03 ± 1.0e-05	1.194e-03 ± 1.5e-05	1.121e-03 ± 2.3e-05	1.214e-03 ± 1.5e-05	1.111e-03 ± 1.4e-05	1.169e-03 ± 4.9e-05
	0.2	3.415e-03 ± 2.5e-05	3.305e-03 ± 3.3e-06	3.475e-03 ± 2.5e-05	3.518e-03 ± 3.6e-05	3.660e-03 ± 2.6e-05	3.430e-03 ± 2.5e-05	3.469e-03 ± 9.4e-05
	0.5	1.226e-02 ± 4.6e-05	1.213e-02 ± 4.7e-05	1.244e-02 ± 4.6e-05	1.256e-02 ± 4.7e-05	1.289e-02 ± 4.6e-05	1.221e-02 ± 4.4e-05	1.241e-02 ± 2.3e-04
	1	2.594e-02 ± 6.2e-05	2.584e-02 ± 1.7e-04	2.627e-02 ± 6.3e-05	2.607e-02 ± 5.0e-05	2.702e-02 ± 6.2e-05	2.602e-02 ± 5.3e-05	2.617e-02 ± 3.5e-04
	2	4.425e-02 ± 7.0e-05	4.396e-02 ± 1.3e-04	4.431e-02 ± 7.0e-05	4.403e-02 ± 5.2e-05	4.535e-02 ± 6.8e-05	4.425e-02 ± 5.0e-05	4.435e-02 ± 4.0e-04
	5	5.103e-02 ± 5.7e-05	5.088e-02 ± 1.1e-04	5.107e-02 ± 5.7e-05	5.064e-02 ± 4.5e-05	5.101e-02 ± 5.6e-05	5.123e-02 ± 3.3e-05	5.101e-02 ± 1.7e-04

Table 4. *OpenDose electron SAFs (kg^{-1}) for the model ICRP 110 adult female, the source Blood Vessels Trunk and target Spleen, Thyroid and Urinary Bladder Wall. SAFs are given for a selection of different Monte Carlo codes and the mean over all available OpenDose data is also shown.*

Target	Energy (MeV)	EGS++ 2018	FLUKA 2011	GATE 8.1	Geant4 10.5	MCNPX 2.7	PENELOPE 2014	OpenDose mean	ICRP 133	diff.
Blood Vessels, Trunk	0.05	2.031e-02 ± 2.4e-05	2.062e-02 ± 2.9e-05	2.047e-02 ± 2.4e-05	2.068e-02 ± 7.2e-05	2.056e-02 ± 2.5e-05	2.047e-02 ± 2.4e-05	2.053e-02 ± 1.1e-04	-	-
	0.1	1.472e-02 ± 1.5e-05	1.496e-02 ± 8.7e-06	1.490e-02 ± 1.5e-05	1.503e-02 ± 4.1e-05	1.496e-02 ± 1.5e-05	1.492e-02 ± 1.4e-05	1.492e-02 ± 8.7e-05	-	-
	0.2	1.320e-02 ± 1.2e-05	1.330e-02 ± 2.0e-05	1.326e-02 ± 1.2e-05	1.328e-02 ± 3.3e-05	1.331e-02 ± 1.2e-05	1.330e-02 ± 1.1e-05	1.328e-02 ± 3.4e-05	-	-
	0.5	1.259e-02 ± 1.4e-05	1.257e-02 ± 1.2e-05	1.255e-02 ± 1.4e-05	1.264e-02 ± 2.1e-05	1.260e-02 ± 1.4e-05	1.259e-02 ± 1.3e-05	1.259e-02 ± 2.3e-05	-	-
	1	1.163e-02 ± 1.5e-05	1.165e-02 ± 3.3e-05	1.154e-02 ± 1.5e-05	1.166e-02 ± 1.3e-05	1.163e-02 ± 1.5e-05	1.162e-02 ± 1.2e-05	1.163e-02 ± 3.5e-05	-	-
	2	1.008e-02 ± 1.5e-05	1.007e-02 ± 2.6e-05	1.009e-02 ± 1.5e-05	1.012e-02 ± 9.4e-06	1.009e-02 ± 1.4e-05	1.011e-02 ± 9.2e-06	1.009e-02 ± 1.7e-05	-	-
	5	7.814e-03 ± 1.2e-05	7.810e-03 ± 2.0e-05	7.813e-03 ± 1.2e-05	7.807e-03 ± 6.6e-06	7.833e-03 ± 1.2e-05	7.826e-03 ± 5.3e-06	7.819e-03 ± 1.0e-05	-	-
Brain	0.05	3.486e-05 ± 4.6e-07	3.026e-05 ± 2.1e-07	3.250e-05 ± 4.4e-07	3.288e-05 ± 1.2e-06	3.110e-05 ± 4.3e-07	3.080e-05 ± 4.0e-07	3.195e-05 ± 1.4e-06	3.091e-05	-3.3%
	0.1	1.122e-04 ± 6.4e-07	1.073e-04 ± 1.6e-07	1.111e-04 ± 6.3e-07	1.113e-04 ± 1.5e-06	1.069e-04 ± 6.2e-07	1.087e-04 ± 5.1e-07	1.095e-04 ± 2.1e-06	1.085e-04	-0.9%
	0.2	1.689e-04 ± 6.7e-07	1.664e-04 ± 4.2e-07	1.681e-04 ± 6.7e-07	1.712e-04 ± 1.5e-06	1.675e-04 ± 6.7e-07	1.678e-04 ± 5.1e-07	1.684e-04 ± 1.4e-06	1.704e-04	1.2%
	0.5	2.734e-04 ± 9.3e-07	2.740e-04 ± 9.1e-07	2.747e-04 ± 9.3e-07	2.705e-04 ± 1.4e-06	2.745e-04 ± 9.3e-07	2.736e-04 ± 7.6e-07	2.737e-04 ± 1.3e-06	2.716e-04	-0.8%
	1	3.686e-04 ± 1.2e-06	3.705e-04 ± 4.2e-07	3.667e-04 ± 1.2e-06	3.740e-04 ± 1.1e-06	3.700e-04 ± 1.2e-06	3.691e-04 ± 9.1e-07	3.700e-04 ± 2.0e-06	3.731e-04	0.8%
	2	4.437e-04 ± 1.4e-06	4.445e-04 ± 1.8e-06	4.433e-04 ± 1.4e-06	4.429e-04 ± 8.8e-07	4.440e-04 ± 1.4e-06	4.425e-04 ± 8.4e-07	4.432e-04 ± 9.7e-07	4.421e-04	-0.2%
	5	4.592e-04 ± 1.5e-06	4.586e-04 ± 1.7e-06	4.604e-04 ± 1.5e-06	4.537e-04 ± 7.2e-07	4.611e-04 ± 1.5e-06	4.617e-04 ± 5.9e-07	4.593e-04 ± 2.7e-06	4.552e-04	-0.9%
Liver	0.05	1.937e-01 ± 2.8e-05	1.983e-01 ± 1.9e-05	1.965e-01 ± 2.8e-05	1.985e-01 ± 6.9e-05	1.981e-01 ± 2.0e-05	1.964e-01 ± 3.1e-05	1.972e-01 ± 1.5e-03	1.590e-01	-19.4%
	0.1	1.105e-01 ± 1.7e-05	1.128e-01 ± 5.0e-06	1.122e-01 ± 1.7e-05	1.128e-01 ± 2.8e-05	1.129e-01 ± 2.3e-05	1.124e-01 ± 1.5e-05	1.124e-01 ± 7.4e-04	8.911e-02	-20.7%
	0.2	1.060e-01 ± 1.5e-05	1.070e-01 ± 1.0e-05	1.068e-01 ± 1.5e-05	1.064e-01 ± 2.4e-05	1.071e-01 ± 1.1e-05	1.069e-01 ± 1.4e-05	1.068e-01 ± 3.7e-04	8.315e-02	-22.1%
	0.5	1.060e-01 ± 1.8e-05	1.063e-01 ± 3.0e-05	1.062e-01 ± 1.8e-05	1.065e-01 ± 2.1e-05	1.063e-01 ± 2.1e-05	1.063e-01 ± 1.7e-05	1.063e-01 ± 1.3e-04	8.222e-02	-22.6%
	1	9.650e-02 ± 1.9e-05	9.652e-02 ± 2.6e-05	9.552e-02 ± 1.9e-05	9.715e-02 ± 2.6e-05	9.653e-02 ± 1.9e-05	9.659e-02 ± 1.5e-05	9.649e-02 ± 4.2e-04	7.317e-02	-24.2%
	2	7.886e-02 ± 1.8e-05	7.888e-02 ± 2.1e-05	7.878e-02 ± 1.8e-05	7.878e-02 ± 2.2e-05	7.867e-02 ± 1.6e-05	7.889e-02 ± 1.1e-05	7.880e-02 ± 7.0e-05	5.971e-02	-24.2%
	5	5.254e-02 ± 1.6e-05	5.264e-02 ± 1.2e-05	5.252e-02 ± 1.6e-05	5.238e-02 ± 1.5e-05	5.228e-02 ± 1.6e-05	5.257e-02 ± 5.7e-06	5.252e-02 ± 1.2e-04	4.089e-02	-22.1%

Table 5. *OpenDose photon SAFs (kg^{-1}) for the model ICRP 110 adult female, the source Liver and target Blood Vessels Trunk, Brain and Liver. SAFs are given for a selection of different Monte Carlo codes and the last 2 columns compare the mean over all available OpenDose data to ICRP 133 data.*

Target	Energy (MeV)	EGS++ 2018	FLUKA 2011	GATE 8.1	Geant4 10.5	MCNPX 2.7	PENELOPE 2014	OpenDose mean	ICRP 133	diff.
Spleen	0.05	1.668e-02 ± 3.0e-05	1.681e-02 ± 2.7e-05	1.690e-02 ± 3.0e-05	1.710e-02 ± 8.9e-05	1.679e-02 ± 3.0e-05	1.679e-02 ± 2.9e-05	1.683e-02 ± 1.2e-04	1.622e-02	-3.6%
	0.1	1.455e-02 ± 2.1e-05	1.481e-02 ± 3.8e-05	1.479e-02 ± 2.1e-05	1.494e-02 ± 5.6e-05	1.486e-02 ± 2.1e-05	1.479e-02 ± 1.9e-05	1.480e-02 ± 1.1e-04	1.481e-02	0.0%
	0.2	1.297e-02 ± 1.7e-05	1.312e-02 ± 1.2e-05	1.307e-02 ± 1.7e-05	1.317e-02 ± 4.3e-05	1.309e-02 ± 1.7e-05	1.309e-02 ± 1.5e-05	1.308e-02 ± 5.3e-05	1.321e-02	1.0%
	0.5	1.230e-02 ± 1.9e-05	1.233e-02 ± 1.4e-05	1.229e-02 ± 1.9e-05	1.235e-02 ± 2.9e-05	1.230e-02 ± 1.8e-05	1.230e-02 ± 1.7e-05	1.231e-02 ± 2.3e-05	1.234e-02	0.3%
	1	1.145e-02 ± 2.0e-05	1.147e-02 ± 3.2e-05	1.133e-02 ± 2.0e-05	1.146e-02 ± 1.8e-05	1.148e-02 ± 2.1e-05	1.145e-02 ± 1.6e-05	1.145e-02 ± 4.5e-05	1.133e-02	-1.0%
	2	1.009e-02 ± 2.1e-05	1.007e-02 ± 1.0e-06	1.008e-02 ± 2.1e-05	1.006e-02 ± 1.3e-05	1.008e-02 ± 2.0e-05	1.011e-02 ± 1.2e-05	1.008e-02 ± 1.5e-05	9.897e-03	-1.8%
	5	7.960e-03 ± 1.8e-05	7.967e-03 ± 1.7e-05	7.962e-03 ± 1.8e-05	7.932e-03 ± 9.2e-06	7.954e-03 ± 1.8e-05	7.945e-03 ± 7.0e-06	7.954e-03 ± 1.3e-05	7.953e-03	-0.0%
Thyroid	0.05	1.833e-03 ± 2.7e-05	1.752e-03 ± 1.4e-05	1.790e-03 ± 2.7e-05	1.922e-03 ± 8.1e-05	1.804e-03 ± 2.7e-05	1.817e-03 ± 2.6e-05	1.813e-03 ± 4.8e-05	1.753e-03	-3.3%
	0.1	2.309e-03 ± 2.2e-05	2.335e-03 ± 7.0e-06	2.326e-03 ± 2.2e-05	2.524e-03 ± 6.7e-05	2.363e-03 ± 2.2e-05	2.355e-03 ± 2.1e-05	2.360e-03 ± 6.4e-05	2.306e-03	-2.3%
	0.2	2.321e-03 ± 1.8e-05	2.326e-03 ± 6.5e-06	2.284e-03 ± 1.8e-05	2.354e-03 ± 5.0e-05	2.276e-03 ± 1.8e-05	2.271e-03 ± 1.7e-05	2.303e-03 ± 2.8e-05	2.353e-03	2.2%
	0.5	2.399e-03 ± 2.1e-05	2.364e-03 ± 1.1e-05	2.424e-03 ± 2.1e-05	2.425e-03 ± 3.6e-05	2.417e-03 ± 2.1e-05	2.445e-03 ± 2.0e-05	2.411e-03 ± 2.3e-05	2.387e-03	-1.0%
	1	2.440e-03 ± 2.4e-05	2.414e-03 ± 2.7e-05	2.438e-03 ± 2.4e-05	2.352e-03 ± 2.4e-05	2.450e-03 ± 2.5e-05	2.418e-03 ± 2.0e-05	2.426e-03 ± 3.3e-05	2.429e-03	0.1%
	2	2.273e-03 ± 2.5e-05	2.326e-03 ± 4.9e-05	2.305e-03 ± 2.5e-05	2.248e-03 ± 1.8e-05	2.331e-03 ± 2.5e-05	2.346e-03 ± 1.7e-05	2.300e-03 ± 3.3e-05	2.350e-03	2.2%
	5	1.937e-03 ± 2.2e-05	1.916e-03 ± 4.2e-06	1.943e-03 ± 2.2e-05	1.833e-03 ± 1.3e-05	1.922e-03 ± 2.2e-05	1.951e-03 ± 1.0e-05	1.916e-03 ± 3.5e-05	1.950e-03	1.8%
Urinary Bladder Wall	0.05	1.652e-04 ± 5.2e-06	1.579e-04 ± 2.1e-06	1.565e-04 ± 5.1e-06	1.287e-04 ± 1.3e-05	1.466e-04 ± 4.9e-06	1.546e-04 ± 5.0e-06	1.531e-04 ± 1.1e-05	1.443e-04	-5.7%
	0.1	4.198e-04 ± 6.0e-06	4.097e-04 ± 1.2e-07	4.159e-04 ± 5.9e-06	4.084e-04 ± 1.7e-05	4.024e-04 ± 5.8e-06	4.114e-04 ± 5.8e-06	4.107e-04 ± 6.2e-06	4.070e-04	-0.9%
	0.2	5.303e-04 ± 5.3e-06	5.297e-04 ± 2.7e-06	5.350e-04 ± 5.3e-06	5.563e-04 ± 1.6e-05	5.346e-04 ± 5.3e-06	5.361e-04 ± 5.1e-06	5.365e-04 ± 7.8e-06	5.302e-04	-1.2%
	0.5	7.117e-04 ± 6.9e-06	7.228e-04 ± 2.8e-06	7.129e-04 ± 6.9e-06	7.175e-04 ± 1.2e-05	7.309e-04 ± 7.0e-06	7.217e-04 ± 6.8e-06	7.197e-04 ± 7.1e-06	6.831e-04	-5.1%
	1	8.795e-04 ± 8.7e-06	8.396e-04 ± 2.2e-06	8.708e-04 ± 8.5e-06	8.753e-04 ± 9.4e-06	8.745e-04 ± 8.6e-06	8.691e-04 ± 7.7e-06	8.695e-04 ± 1.2e-05	8.949e-04	2.9%
	2	9.621e-04 ± 8.9e-06	9.734e-04 ± 6.3e-06	9.637e-04 ± 8.9e-06	9.637e-04 ± 7.3e-06	9.568e-04 ± 8.7e-06	9.531e-04 ± 6.9e-06	9.596e-04 ± 6.8e-06	9.755e-04	1.7%
	5	9.132e-04 ± 7.2e-06	9.205e-04 ± 3.8e-06	9.126e-04 ± 7.3e-06	9.224e-04 ± 5.9e-06	9.253e-04 ± 7.2e-06	9.204e-04 ± 4.7e-06	9.198e-04 ± 4.2e-06	9.187e-04	-0.1%

Table 6. *OpenDose photon SAFs (kg^{-1}) for the model ICRP 110 adult female, the source Liver and target Spleen, Thyroid and Urinary Bladder Wall. SAFs are given for a selection of different Monte Carlo codes and the last 2 columns compare the mean over all available OpenDose data to ICRP 133 data.*

Target	Energy (MeV)	EGS++ 2018	FLUKA 2011	GATE 8.1	Geant4 10.5	MCNPX 2.7	PENELOPE 2014	OpenDose mean	ICRP 133	diff.
Blood Vessels, Trunk	0.05	1.789e-05 ± 7.2e-07	3.802e-05 ± 1.1e-04	1.687e-05 ± 7.1e-07	1.796e-05 ± 1.3e-06	1.773e-05 ± 7.1e-07	1.873e-05 ± 7.5e-07	1.984e-05 ± 6.9e-06	-	-
	0.1	5.311e-05 ± 1.2e-06	6.910e-05 ± 5.9e-07	5.745e-05 ± 1.3e-06	5.644e-05 ± 2.2e-06	5.900e-05 ± 1.3e-06	2.947e-05 ± 1.0e-06	5.431e-05 ± 1.0e-05	-	-
	0.2	1.603e-04 ± 2.1e-06	1.701e-04 ± 5.1e-07	1.622e-04 ± 2.1e-06	1.619e-04 ± 3.2e-06	1.711e-04 ± 2.2e-06	1.563e-04 ± 2.1e-06	1.634e-04 ± 4.8e-06	-	-
	0.5	5.640e-04 ± 3.9e-06	5.769e-04 ± 8.9e-06	5.708e-04 ± 4.0e-06	5.729e-04 ± 4.0e-06	5.958e-04 ± 4.1e-06	5.560e-04 ± 3.7e-06	5.722e-04 ± 1.1e-05	-	-
	1	1.295e-03 ± 5.8e-06	1.300e-03 ± 5.8e-06	1.305e-03 ± 5.8e-06	1.263e-03 ± 4.5e-06	1.343e-03 ± 5.9e-06	1.289e-03 ± 4.8e-06	1.299e-03 ± 2.2e-05	-	-
	2	3.092e-03 ± 8.7e-06	3.112e-03 ± 1.2e-05	3.115e-03 ± 8.7e-06	3.095e-03 ± 5.5e-06	3.251e-03 ± 8.8e-06	3.090e-03 ± 5.3e-06	3.114e-03 ± 5.3e-05	-	-
	5	1.005e-02 ± 1.5e-05	1.012e-02 ± 7.4e-05	1.004e-02 ± 1.5e-05	1.008e-02 ± 7.3e-06	1.050e-02 ± 1.5e-05	1.011e-02 ± 6.0e-06	1.012e-02 ± 1.5e-04	-	-
Brain	0.05	0.0 ± 0.0	0.0 ± 0.0	0.0 ± 0.0	0.0 ± 0.0	0.0 ± 0.0	0.0 ± 0.0	0.0 ± 0.0	0.0	-
	0.1	8.427e-09 ± 6.5e-09	1.471e-08 ± 3.4e-09	2.067e-09 ± 1.1e-09	0.0e00 ± 0.0e00	5.755e-09 ± 3.9e-09	5.432e-09 ± 3.1e-09	6.563e-09 ± 4.3e-09	0.0	-
	0.2	3.136e-08 ± 7.6e-09	3.091e-08 ± 3.8e-09	3.029e-08 ± 6.9e-09	3.164e-08 ± 1.4e-08	2.285e-08 ± 5.5e-09	4.771e-08 ± 8.0e-09	3.193e-08 ± 7.8e-09	6.655e-08	108.5%
	0.5	1.634e-07 ± 1.3e-08	1.355e-07 ± 3.4e-08	1.705e-07 ± 1.4e-08	1.679e-07 ± 3.2e-08	1.757e-07 ± 1.4e-08	1.521e-07 ± 1.0e-08	1.635e-07 ± 1.3e-08	1.650e-07	0.9%
	1	4.694e-07 ± 2.2e-08	4.736e-07 ± 1.7e-08	5.037e-07 ± 2.2e-08	4.520e-07 ± 3.7e-08	4.940e-07 ± 2.2e-08	4.631e-07 ± 1.7e-08	4.777e-07 ± 1.8e-08	5.057e-07	5.8%
	2	1.509e-06 ± 4.2e-08	1.367e-06 ± 3.2e-08	1.507e-06 ± 4.1e-08	1.507e-06 ± 4.7e-08	1.491e-06 ± 4.0e-08	1.498e-06 ± 3.1e-08	1.478e-06 ± 4.4e-08	1.605e-06	8.6%
	5	6.099e-06 ± 8.8e-08	6.244e-06 ± 3.4e-07	6.113e-06 ± 8.7e-08	6.076e-06 ± 6.5e-08	6.257e-06 ± 8.7e-08	6.072e-06 ± 5.3e-08	6.149e-06 ± 9.6e-08	5.870e-06	-4.5%
Liver	0.05	7.139e-01 ± 1.4e-06	7.133e-01 ± 0.0e+00	7.139e-01 ± 1.4e-06	7.139e-01 ± 5.8e-05	7.139e-01 ± 0.0e+00	7.139e-01 ± 7.1e-05	7.138e-01 ± 2.0e-04	5.522e-01	-22.6%
	0.1	7.130e-01 ± 2.5e-06	7.127e-01 ± 3.7e-06	7.130e-01 ± 2.6e-06	7.130e-01 ± 1.4e-04	7.129e-01 ± 0.0e+00	7.136e-01 ± 7.1e-05	7.130e-01 ± 2.3e-04	5.514e-01	-22.7%
	0.2	7.105e-01 ± 4.3e-06	7.103e-01 ± 2.8e-06	7.105e-01 ± 4.3e-06	7.105e-01 ± 2.0e-04	7.103e-01 ± 0.0e+00	7.105e-01 ± 6.9e-05	7.105e-01 ± 8.9e-05	5.492e-01	-22.7%
	0.5	7.011e-01 ± 7.9e-06	7.009e-01 ± 5.5e-06	7.010e-01 ± 7.9e-06	7.011e-01 ± 2.1e-04	7.005e-01 ± 0.0e+00	7.012e-01 ± 6.0e-05	7.010e-01 ± 2.1e-04	5.423e-01	-22.6%
	1	6.859e-01 ± 1.1e-05	6.857e-01 ± 1.3e-05	6.857e-01 ± 1.1e-05	6.859e-01 ± 2.1e-04	6.847e-01 ± 0.0e+00	6.860e-01 ± 4.7e-05	6.857e-01 ± 3.9e-04	5.284e-01	-22.9%
	2	6.577e-01 ± 1.5e-05	6.577e-01 ± 5.6e-05	6.575e-01 ± 1.5e-05	6.578e-01 ± 2.0e-04	6.555e-01 ± 0.0e+00	6.578e-01 ± 3.2e-05	6.574e-01 ± 7.4e-04	5.055e-01	-23.1%
	5	5.804e-01 ± 2.1e-05	5.812e-01 ± 7.0e-05	5.807e-01 ± 2.1e-05	5.810e-01 ± 1.8e-04	5.758e-01 ± 0.0e+00	5.802e-01 ± 1.9e-05	5.801e-01 ± 1.7e-03	4.499e-01	-22.4%

Table 7. *OpenDose electron SAFs (kg^{-1}) for the model ICRP 110 adult female, the source Liver and target Blood Vessels Trunk, Brain and Liver. SAFs are given for a selection of different Monte Carlo codes and the last 2 columns compare the mean over all available OpenDose data to ICRP 133 data.*

Target	Energy (MeV)	EGS++ 2018	FLUKA 2011	GATE 8.1	Geant4 10.5	MCNPX 2.7	PENELOPE 2014	OpenDose mean	ICRP 133	diff.
Spleen	0.05	6.004e-07 ± 1.6e-07	6.899e-07 ± 1.4e-05	5.851e-07 ± 1.7e-07	5.154e-07 ± 4.8e-07	8.723e-07 ± 2.0e-07	6.104e-07 ± 1.6e-07	6.002e-07 ± 1.4e-07	2.016e-07	-66.4%
	0.1	2.739e-06 ± 2.6e-07	3.119e-06 ± 4.3e-07	3.051e-06 ± 2.8e-07	2.829e-06 ± 9.0e-07	3.498e-06 ± 3.0e-07	1.544e-06 ± 1.9e-07	2.955e-06 ± 6.6e-07	2.540e-06	-14.0%
	0.2	8.369e-06 ± 3.4e-07	8.778e-06 ± 2.3e-07	7.429e-06 ± 3.1e-07	9.856e-06 ± 1.1e-06	8.983e-06 ± 3.5e-07	8.677e-06 ± 3.3e-07	8.513e-06 ± 7.4e-07	8.631e-06	1.4%
	0.5	2.109e-05 ± 3.8e-07	2.297e-05 ± 3.6e-07	2.138e-05 ± 4.0e-07	1.861e-05 ± 9.3e-07	2.247e-05 ± 4.0e-07	2.139e-05 ± 3.6e-07	2.166e-05 ± 1.3e-06	2.170e-05	0.2%
	1	4.240e-05 ± 5.1e-07	4.340e-05 ± 7.1e-07	4.330e-05 ± 5.2e-07	4.139e-05 ± 1.0e-06	4.455e-05 ± 5.1e-07	4.254e-05 ± 4.6e-07	4.275e-05 ± 9.1e-07	4.584e-05	7.2%
	2	8.592e-05 ± 7.6e-07	9.082e-05 ± 2.1e-06	8.824e-05 ± 7.7e-07	8.710e-05 ± 1.1e-06	9.105e-05 ± 7.6e-07	8.538e-05 ± 6.1e-07	8.769e-05 ± 2.0e-06	9.108e-05	3.9%
	5	2.263e-04 ± 1.4e-06	2.263e-04 ± 3.9e-06	2.253e-04 ± 1.3e-06	2.156e-04 ± 1.2e-06	2.334e-04 ± 1.3e-06	2.248e-04 ± 8.6e-07	2.253e-04 ± 4.5e-06	2.250e-04	-0.1%
Thyroid	0.05	0.000e+00 ± 0.0e+00	1.478e-09 ± 1.5e-07	0.000e+00 ± 0.0e+00	0.000e+00 ± 0.0e+00	0.000e+00 ± 0.0e+00	0.000e+00 ± 0.0e+00	1.847e-10 ± 5.2e-10	0.000e+00	-100.0%
	0.1	9.424e-08 ± 4.9e-08	2.078e-07 ± 2.1e-07	4.172e-08 ± 2.9e-08	0.000e+00 ± 0.0e+00	3.439e-07 ± 2.6e-07	8.770e-08 ± 5.2e-08	1.314e-07 ± 1.2e-07	2.896e-07	120.2%
	0.2	7.255e-07 ± 2.8e-07	1.069e-06 ± 4.9e-07	1.148e-06 ± 3.6e-07	6.556e-07 ± 6.0e-07	9.704e-07 ± 3.1e-07	1.276e-06 ± 4.2e-07	1.031e-06 ± 3.1e-07	8.380e-07	-18.7%
	0.5	2.783e-06 ± 3.5e-07	3.704e-06 ± 1.3e-07	3.657e-06 ± 4.4e-07	5.123e-06 ± 1.3e-06	3.587e-06 ± 4.6e-07	2.453e-06 ± 3.4e-07	3.290e-06 ± 8.6e-07	1.874e-06	-43.0%
	1	6.276e-06 ± 4.7e-07	8.215e-06 ± 1.4e-06	7.256e-06 ± 5.0e-07	6.587e-06 ± 1.3e-06	6.903e-06 ± 5.6e-07	7.300e-06 ± 5.1e-07	7.077e-06 ± 5.9e-07	8.355e-06	18.1%
	2	1.713e-05 ± 1.0e-06	1.672e-05 ± 1.7e-06	1.470e-05 ± 7.5e-07	1.347e-05 ± 1.2e-06	1.500e-05 ± 7.8e-07	1.628e-05 ± 8.7e-07	1.534e-05 ± 1.2e-06	1.637e-05	6.7%
	5	4.218e-05 ± 1.4e-06	3.855e-05 ± 4.0e-06	4.452e-05 ± 1.6e-06	4.621e-05 ± 1.5e-06	4.472e-05 ± 1.5e-06	4.499e-05 ± 1.1e-06	4.380e-05 ± 2.3e-06	3.874e-05	-11.6%
Urinary Bladder Wall	0.05	0.000e+00 ± 0.0e+00	0.000e+00 ± 0.0e+00	0.000e+00 ± 0.0e+00	0.000e+00 ± 0.0e+00	0.000e+00 ± 0.0e+00	0.000e+00 ± 0.0e+00	0.000e+00 ± 0.0e+00	0.000e+00	-
	0.1	2.969e-08 ± 2.2e-08	9.194e-08 ± 9.2e-08	4.910e-08 ± 4.5e-08	0.000e+00 ± 0.0e+00	4.153e-18 ± 2.2e-18	0.000e+00 ± 0.0e+00	2.430e-08 ± 3.3e-08	0.000e+00	-100.0%
	0.2	6.160e-08 ± 2.7e-08	2.447e-07 ± 1.3e-07	1.069e-07 ± 6.8e-08	0.000e+00 ± 0.0e+00	1.843e-07 ± 9.1e-08	1.271e-07 ± 5.2e-08	1.414e-07 ± 7.2e-08	1.086e-07	-23.2%
	0.5	4.236e-07 ± 1.2e-07	5.559e-07 ± 8.0e-08	5.103e-07 ± 8.9e-08	8.154e-07 ± 2.8e-07	5.879e-07 ± 1.1e-07	5.155e-07 ± 9.6e-08	5.753e-07 ± 1.2e-07	5.907e-07	2.7%
	1	1.410e-06 ± 1.7e-07	1.199e-06 ± 4.4e-08	1.676e-06 ± 1.8e-07	8.475e-07 ± 2.5e-07	1.514e-06 ± 1.5e-07	1.464e-06 ± 1.6e-07	1.407e-06 ± 2.5e-07	1.618e-06	15.0%
	2	4.418e-06 ± 3.4e-07	5.469e-06 ± 1.7e-06	4.055e-06 ± 3.0e-07	3.626e-06 ± 3.9e-07	3.660e-06 ± 2.4e-07	3.795e-06 ± 2.4e-07	4.167e-06 ± 5.6e-07	4.189e-06	0.5%
	5	1.446e-05 ± 5.4e-07	1.388e-05 ± 1.9e-06	1.414e-05 ± 5.1e-07	1.379e-05 ± 5.3e-07	1.532e-05 ± 5.7e-07	1.517e-05 ± 4.6e-07	1.450e-05 ± 6.7e-07	1.415e-05	-2.4%

Table 8. *OpenDose electron SAFs (kg^{-1}) for the model ICRP 110 adult female, the source Liver and target Spleen, Thyroid and Urinary Bladder Wall. SAFs are given for a selection of different Monte Carlo codes and the last 2 columns compare the mean over all available OpenDose data to ICRP 133 data.*